Journal of Metals, Materials and Minerals, Vol. 32, No. 3, pp. 80-85, 2022

Synthesis of $CaCu_3Ti_4O_{12}$ utilizing eggshell waste as a calcium source: Structure, morphology, and dielectric properties

Akhiruddin MADDU[1,*], Habiburahmat YULWAN[1], Irmansyah IRMANSYAH[1], Ahmad Sofyan SULAEMAN[2], and Permono Adi PUTRO[2]

[1] *Department of Physics, IPB University, Jl Meranti Gedung Wing S, Kampus Dramaga, Bogor 16680, Indonesia*
[2] *Department of Physics, Faculty of Science, Universitas Mandiri, Subang, West Java, Indonesia*

***Corresponding author e-mail:** akhiruddin@apps.ipb.ac.id

Received date:
23 April 2022
Revised date
30 June 2022
Accepted date:
4 August 2022

Keywords:
Annealing;
$CaCu_3Ti_4O_{12}$;
Dielectric constant;
Dielectric loss;
Eggshell

Abstract

Calcium copper titanate ($CaCu_3Ti_4O_{12}$, CCTO) has been synthesized utilizing eggshell waste as a source of calcium through the hydrothermal route, followed by annealing treatment at temperatures 950°C and 1050°C. The sample with annealing temperatures of 950°C and 1050°C is named CTO-A and CCTO-B, respectively. The structure, microstructure, and dielectric properties of CCTO samples were investigated. The X-ray diffraction analysis results confirmed that the pure phase of CCTO has been successfully synthesized as identified in the diffraction pattern. The average crystallite size of CCTO is quite large due to annealing at high-temperature. The morphology of CCTO by electron microscopy investigation showed the grains tends to agglomerate as the annealing temperature increases due to the solid-state diffusion. Dielectric property investigation showed the CCTO samples have a high dielectric constant at low frequencies and decrease with increasing frequency. Sample CCTO-A annealed at 950ºC has a higher dielectric constant than sample CCTO-B annealed at 1050ºC, otherwise, it has a lower tangent loss than the sample CCTO-B.

1. Introduction

Studies on the properties of calcium-copper-titanate ($CaCu_3Ti_4O_{12}$, CCTO) have been progressing very rapidly in recent decades, and it is because of its unique characteristics and promising technological applications. CCTO is well known as a dielectric material with high relative permittivity or dielectric constant and low dielectric loss, which is called giant dielectrics material [1-4]. Dielectric properties of CCTO are a characteristic that is most studied and investigated to explore its potential applications in electronics technology, including in energy storage devices [5], capacitors [6], gas sensors [7], random access memory [8], and microwave devices [9]. CCTO is also used as a photoanode for photocatalysis and photoelectrocatalysis in solar energy conversion [10]. Despite these significant advances, CCTO's technological applications are limited by its high dielectric loss, which is linked to its grain boundary conductivity [11]. Dielectric permittivity is directly proportional to dielectric loss, which is related to leakage current [12].

Various methods have been developed to synthesize CCTO, each of which has its advantages and disadvantages. The solid-state reaction is a simple method that is most often performed to synthesize CCTO because of easy to be carried out [13-16]. However, in the solid-state reaction, it is difficult to control the crystal phase and the homogeneous microstructure of CCTO. On the other hand, the electrical properties of dielectric ceramics can be improved when these ceramics have a homogeneous microstructure and a pure crystal phase. The sol-gel method is also commonly used to synthesize CCTO, but this method uses more reagents and complex routes than other methods [6,7,17-20]. In addition, other synthesis methods have also been developed to synthesize CCTO, including liquid-phase annealing [21], co-precipitation [22], microwave-assisted process [23], and hydrothermal route [24]. The hydrothermal method has advantages over other methods for various reasons, such as a homogeneous granularity and high crystallinity of produced powder [25].

Nowadays, CCTO is mostly synthesized utilizing commercial metal salts [18,26,27], metal oxides [28-30], and metalorganics [31-33] as starting materials. An alternative source of calcium to synthesize CCTO can utilize natural materials containing high calcium, such as eggshells. High calcium content in calcium carbonate ($CaCO_3$) compounds makes eggshells a commodity that has the potential as a calcium source to synthesize calcium-based dielectric material including $CaTiO_3$ [34-36] and $Ca_{10}(PO_4)_6(OH)_2$ [37-39]. Utilizing eggshells as calcium sources to synthesize CCTO has not yet been reported. The utilization of eggshell waste as a source of calcium in synthesizing CCTO has advantages, including reducing the cost of production and minimalizing the waste's environmental impact [40].

In this study, the eggshell waste was utilized as a calcium source to synthesize giant dielectric material CCTO. Synthesis of CCTO utilizing eggshell waste as a calcium source is still rarely done before. The use of eggshell waste is aimed at reducing the environmental impact it causes and producing functional materials that will add added value. In this work, CCTO was synthesized by the hydrothermal

method, where the reaction occurs in a hydrothermal reactor under high pressure, then proceed with annealing treatment to produce CCTO crystals. The effect of annealing treatment on crystal properties, microstructure, and dielectric properties of produced CCTO samples was studied. Specifically, the purity of the phase was investigated, and lattice parameters, crystal size, and grain interface were also investigated due to annealing treatment and its effect on the dielectric constant and dielectric loss (tan δ) of CCTO samples.

2. Experimental procedures

2.1 Preparation of $CaCO_3$ from eggshells

Eggshells collected from cooking wastes were washed with distilled water to remove macro contaminants, then dried in air. Dry eggshells were calcined at 800°C for 5 h in a furnace with 5°C·min^{-1} heating rates. The product of the calcination process is ground in a mortar by pestle to obtain white $CaCO_3$ powder.

2.2 Synthesis of CCTO

CCTO is prepared through a three-stage process. CCTO was synthesized from three starting materials; namely, $CaCO_3$ powder derived from eggshell, $Cu(NO_3)_2$, and TiO_2 powder (Degussa P25). First, $CaCO_3$ (1.14 g), $Cu(NO_3)_2$ (4.83 g), and TiO_2 powders (1.59 g) were mixed and dissolved in 100 L of NaOH (0.1 M) solution. The mixed solution was continuously stirred at 1000 rpm for 30 min by a magnetic stirrer, then poured into the autoclave to be processed via the hydrothermal treatment. The hydrothermal treatment was carried out by heating the autoclave at 250°C for 24 h to achieve a high pressure within the reactor. The product of the hydrothermal treatment is a solution with brown precipitate. The precipitate was washed with the alcohol solution (97%) and distilled water, and this step was carried out three times alternately. The precipitate was filtered and dried in an air atmosphere at a temperature of 80°C to obtain dry CCTO powder. Second, the brown powder was calcined at 900°C in a furnace for 8 h, then ground in a mortar by pestle to obtain a finer powder. Finally, CCTO powder was divided into two with the same weight and formed into pellets with 1.21 cm diameter and 0.23 cm thickness. Two obtained pellets were annealed at 950°C and 1050°C for 12 h in a furnace. The sample with 950°C and 1050°C is named CCTO-A and CCTO-B, respectively. These annealed temperatures triggered a chemical reaction as shown in equation (1) on the resulting CCTO:

$$CaCO_3 + 3CuO + 4TiO_2 \rightarrow CaCu_3Ti_4O_{12} + CO_2 \qquad (1)$$

2.3 Characterization of CCTO

The CCTO samples characterized their crystal properties, microstructure, and dielectric properties. Crystal properties were investigated by X-Ray diffraction analysis using the GBC Emma (enhanced multi-materials analyzer) X-ray diffractometer (XRD). The X-ray diffractogram was analyzed to investigate the crystal properties of CCTO samples, including their crystal phase, lattice parameter, and average crystallite size (ACS). The surface morphology of CCTO was taken using a scanning electron microscope (SEM) then the microstructure was explored, including grain distribution and inter-grain diffusion. Investigation of dielectrics properties of CCTO was carried out by using LCR Meter (Hioki Hi-Tester 3522-50) to obtain capacitance-frequency curves. Capacitance value was measured in the frequency range at 10^2 Hz to 10^4 Hz at an oscillation voltage of 100 mV and room temperature, then the dielectric constant (relative permittivity) and dielectric loss (tangent loss) in the frequency range was determined.

3. Results and discussion

3.1 Crystal properties

The XRD analysis is conducted to ensure the crystal phase, lattice parameters, and average crystallite size (ACS) of CCTO samples annealed at different temperatures, 950°C (CCTO-A) and 1050°C (CCTO-B). The X-ray diffractogram of CCTO-A and CCTO-B is shown in Figure 1. Based on the diffraction pattern, both samples have a pure phase of CCTO crystal, there were no other phases originating from starting materials such as CaO from eggshell, CuO, and TiO_2. Also, there are no secondary phases formed, such as $CaTiO_3$, CuO, and Cu_2O, coming from the reaction process in each synthesis step. These have been confirmed on major diffraction peaks that have *hkl* values (211), (220), (310), (222), (321), (400), (411), (332), (442), and (440), respectively. The diffraction peaks match to the cubic-perovskite structure of CCTO corresponding to JCPDS card no. 75-2188 [41]. These results confirm that CCTO formation can effectively occur in the temperature range from 850°C to 1120°C as in previous studies [18,42].

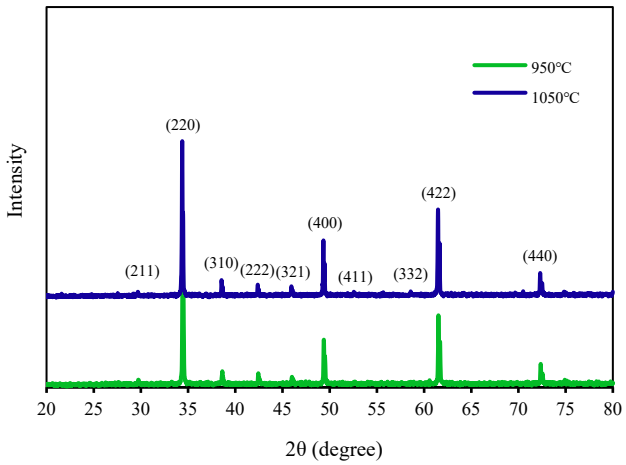

Figure 1. X-Ray diffractogram of CCTO samples annealed at 950°C and 1050°C.

Table 1. Average crystal size (ACS) of CCTO-A and CCTO-B samples annealed at 950°C and 1050°C, respectively.

Samples	FWHM (rad)	ACS (Å)
CCTO-A	0.00402	377.545
CCTO-B	0.00398	380.414

Meanwhile, there is no significant contrast between diffraction patterns of CCTO-A and CCTO-B samples, except the diffraction peaks of CCTO-B (annealed at 1050°C) are higher than CCTO-A (annealed at 950°C) peaks. The lattice parameters of CCTO samples were calculated by using Cohen's method [43]. CCTO have a cubic-perovskite crystal structure with parameter values a = b = c. The calculation results found the lattice parameters were 7.425 Å and 7.455 Å for CCTO-A and CCTO-B, respectively. The lattice parameter slightly increased with increasing temperature from 950°C to 1050°C. Increasing the annealing temperature possibly results in the atomic level diffusion that affects the stretching of the distance between the atoms and enlarges the lattice parameters [18,42]. Therefore, there is a slight increase in lattice parameter due to the increasing annealing temperature.

Furthermore, the average crystallite size (ACS) of CCTO samples was determined using Scherrer method based on values of Full-Width at Half Maximum (FWHM) for each peak of CCTO samples in the diffraction pattern. Debye-Scherrer's formula is given by equation (2) as follows [44]:

$$D = 0.9\,\lambda/\beta \cos\theta \quad (2)$$

where D is the ACS value, λ is the wavelength of X-ray from copper as an X-ray source (λ_{Cu} = 1.5406 Å), β is the FWHM value (in radian) from peak widening, and θ is the diffraction angle. The calculation results of the ACS value are summarized in Table 1. The annealing temperature significantly affected the FWHM value, so which also affected the ACS values of CCTO. Increasing the annealing temperature resulted in the diffraction spectrum becoming narrower; thus, the FWHM value was smaller, resulting in the ACS value being larger. Generally, the ACS value of CCTO is greater than 300 Å, which corresponds to a sharp and narrow diffraction peak. The relatively large ACS value is due to the high annealing temperature, this is because the distance between the atoms in the crystal expands [44].

3.2 Morphology

The surface morphology images of the CCTO were recorded using the scanning electron microscope (SEM) apparatus. Figure 2 shows the SEM images of the surface morphology of CCTO samples (CCTO-A and CCTO-B). In general, CCTO samples have a micro-structure with interconnected grains. This is possible because the heating temperature is quite high which results in solid diffusion in the CCTO samples so that the grains coalesce.

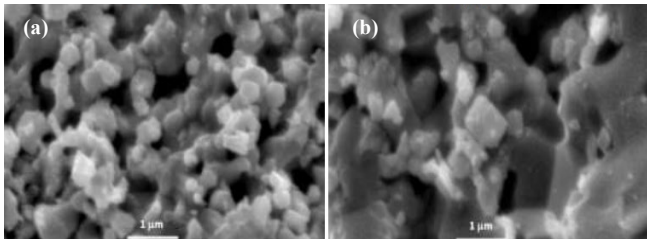

Figure 2. SEM images of CCTO samples annealed at (a) 950°C and (b) 1050°C.

Sample CCTO-A annealed at 950°C has a microstructure with granules that start to coalesce but still show a cube-shaped grain with an average size of around 0.3 µm. This coalescence of grains occurs through diffusion between grains due to the high temperature of the annealing treatment. The image of morphology shows the microstructure with the grains starting to merge with each other, although the grains can still be identified. This phenomenon usually occurs in the material processed at high temperatures. It was reported that the morphology changed significantly with different annealing temperatures [45].

The solid-state diffusion was more evident in the sample CCTO-B annealed at 1050°C, in which the grains almost completely fused in the sample, and even tended to start to melt. In the image it appears that almost all the grains have coalesced, the inter-grain boundary mostly cannot be observed, although some grains still have grain boundaries. In the CCTO-B sample, the stronger inter-grain diffusion has been occurred due to the higher temperature in heating treatment. Consequently, the grains more merged even mostly have been melted.

3.3 Dielectric properties

The study of dielectric properties is based on an interaction between the electric field and materials. These interactions result in polarization of the electric charges in order to compensate for the electric field applied to the material, that is the positive and negative charges move in opposite directions. Each of polarization mechanism possesses its own limiting frequency or depends on the frequency.

The properties of dielectric materials are characterized by their relative permittivity, dielectric loss, and dielectric strength. Permittivity is a material property that affects the Coulomb force between two point charges in the material. The relative permittivity (ε_r) or dielectric constant (κ) is the factor of decreasing the electric field between charges relative to a vacuum. The relative permittivity (ε_r) is defined as the ratio of the permittivity of material ε(ω) to the permittivity of vacuum (ε_o), as follow

$$\varepsilon_r(\omega) = \varepsilon(\omega)/\varepsilon_o \quad (3)$$

where ε(ω) is the complex frequency-dependent permittivity of the material, and ε_o is the vacuum permittivity (8.854×10^{-12} F·m^{-2}). Relative permittivity is a dimensionless number that is in general complex-valued; its real and imaginary parts are denoted as

$$\varepsilon_r(\omega) = \varepsilon'_r(\omega) - i\varepsilon''_r(\omega) \quad (4)$$

where ε′(ω) and ε″(ω) are real and imaginary parts of the complex permittivity $\varepsilon_r(\omega)$ as a function of frequency. While the dielectric loss tangent is defined as

$$\tan\delta = \varepsilon''/\varepsilon' \quad (5)$$

Dielectric properties were studied to investigate the polarization ability of CCTO under an applied electric field at room temperature. Figure 3 depicts the relative permeability (ε_r) of CCTO-A and CCTO-B dependent on frequency. In general, the relative permittivity of CCTO samples is quite high, above 3000, even CCTO-A sample heated at 950°C have relative permittivity above 25,000 at low frequencies.

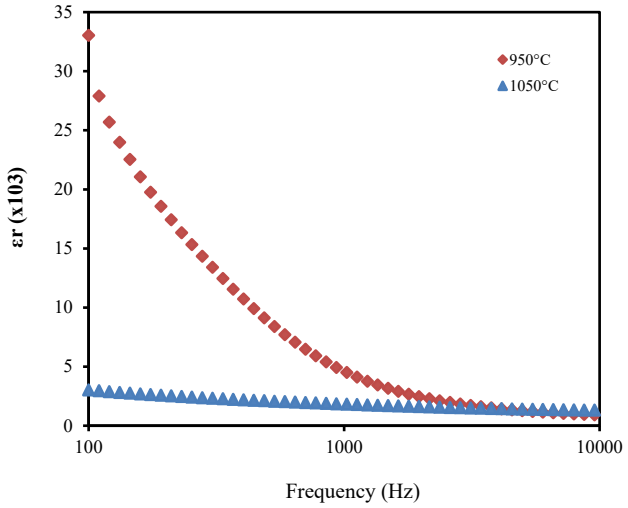

Figure 3. The dielectric constant depends on frequency of CCTO samples annealed at 950°C and 1050°C.

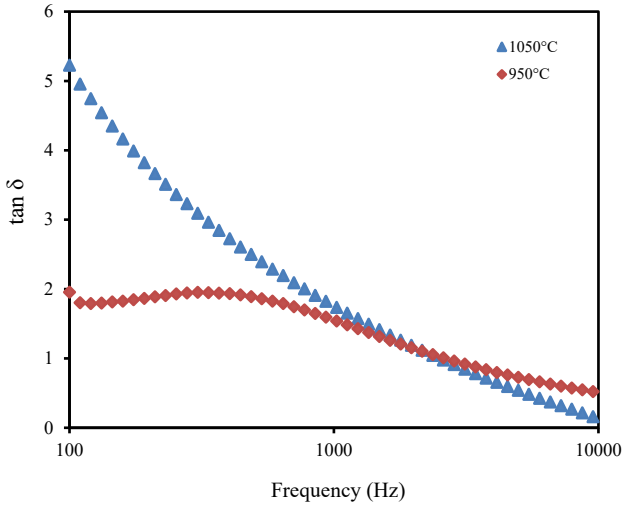

Figure 4. The dielectric loss (tan δ) depends on the frequency of CCTO samples annealed at 950°C and 1050°C.

These results indicate that samples synthesized utilize eggshells as a calcium source and can produce giant dielectric materials. The high ε_r values are shown by CCTO-A at low frequency even though it decreases gradually at a higher frequency. This result relates to the strong polarization of CCTO that makes the current move under an external electric field to form a dipole in low frequency; thus, it means that charge carriers are accumulated in the semiconducting and insulating grain boundary interface [46]. Moreover, the ε_r values were obtained due to the electrons congregating around the crystal boundary of CCTO to form a strong interfacial polarization based on the internal barrier layer capacitor model [18,41].

Meanwhile, a lowering of ε_r values at a higher frequency due to relaxation polarization of CCTO. When the frequency of the electric field increases to a certain value, and beyond their relaxation frequency, in this situation, the movement of the dipole cannot respond to the change of the electric field direction reversal timely. Therefore, at high frequency, the dipole polarization is greatly weakened, and the dipole rotation needs to overcome resistance in the material [47].

Furthermore, the ε_r values are smaller in CCTO-B than CCTO-A. The frequency of the electric field may cause it to be more than the frequency relaxation of CCTO-B, thus it resulting in low dipole mobility [24]. However, the ε_r of CCTO-B is more stable at a higher frequency than CCTO-A. Prakash *et al* reported that a lower of ε_r relates with thinning down of outer surface in CCTO [48]. This is due to the segregation of Cu in the annealing process and oxidation near the surface, which are contributing to the polarization of CCTO [41,48]. Therefore, it results in a lower of ε_r at low frequency but helps polarization stability this CCTO at a higher frequency.

On the other hand, Figure 4 shows a dielectric loss (tan δ) at room temperature, which is determined to understand the energy-loss behavior of the samples [46]. CCTO-A sample resulted in a low tan δ at low frequency, whereas CCTO-B has a higher tan δ at low temperature. This means that CCTO-A has a higher polarization loss than CCTO-B in the low-frequency region. CCTO-B has a peak at an intermediate frequency, indicating a relaxation peak due to orientation polarization resulting from oxygen defects [46]. In previous reports, CCTO is suitable for capacitor applications when it has tan δ below 0.05 at low frequency [18,49]. In this case, CCTO-A and CCTO-B presented higher tan δ above 1.5 at low frequency, resulting in unsuitable for further application.

4. Conclusions

CCTO was successfully produced by a hydrothermal method utilizing eggshell as calcium source followed annealing treatment at 950°C and 1050°C. Both CCTO samples either annealed at 950°C (CCTO-A) or 1050°C (CCTO-B) showed the single-phase crystal structure that was confirmed by x-ray diffraction pattern analysis. SEM images revealed the cube-shaped grains of CCTO-A starting to diffuse each other with an average size of around 0.3 μm. In contrast, CCTO-B resulted in stronger inter-grain diffusion that triggered the grains to merge more agglomerated and the cubic-shaped grains tend to melt. The relative permittivity of CCTO-A (annealed at 950°C) is greater than CCTO-B (annealed at 1050°C). In this case, CCTO-A and CCTO-B present a tan δ greater than 1.5 at low frequencies, making them unsuitable for further applications. Thus, this study still has the opportunity to continue to obtain a tan δ value below 1.5 at the frequency. As a result, CCTO has many potentials, and one of them is a capacitor.

Acknowledgements

The authors thank the operators of the Nanotechnology Laboratory, Center for Agricultural Postharvest Research and Development, Ministry of Agriculture of the Republic of Indonesia for their facilitation for XRD and SEM characterization.

References

[1] P. Mao, J. Wang, P. Xiao, L. Zhang, F. Kang, and H. Gong, "Colossal dielectric response and relaxation behavior in novel system of Zr^{4+} and Nb^{5+} Co-substituted $CaCu_3Ti_4O_{12}$ Ceramics," *Ceramics International,* vol. 47, no. 1, pp. 111-120, 2021.

[2] U. M. Meshiya, P. Y. Raval, N. P. Josh, N. H. Vasoya, P. K. Jha, and K. B. Modi, "Probing fano resonance, relaxor ferroelectricity, light scattering by orbital exchange-bond, orbitons by raman spectroscopy, and their correlation with dielectric properties of pure and Fe^{3+}–substituted calcium-copper-titanate," *Vibrational Spectroscopy,* vol. 112, p. 103201, 2021.

[3] G. Miao, M. Yin, P. Li, J. Hao, W. Li, J. Du, G. Li, C. Wang, and P. Fu, "Effect of Cr Addition on the Structure and Electrical Properties of $CaCu_3Ti_4O_{12}$ NTC Thermistor," *Journal of Alloys and Compounds,* vol. 884, p. 161066, 2021.

[4] H. Moreno, H. Moreno, J. A. Cortes, F. M. Praxedes, S. M. Freitas, M. V. S. Rezende, A. Z. Simoes, V. C. Teixeira, and M. A. Ramirez, "Tunable photoluminescence of $CaCu_3Ti_4O_{12}$ based ceramics modified with tungsten," *Journal of Alloys and Compounds,* vol. 850, p. 156652, 2021.

[5] J-W. Lee and J-H. Koh, "Enhanced dielectric properties of Ag-doped CCTO ceramics for energy storage devices," *Ceramics International,* vol. 43, pp. 9493-9497, 2017.

[6] V. S Puli, S. Adireddy, M. Kothakonda, R. Elupula, and D. B. Chrisey, "Low temperature annealed giant dielectric permittivity $CaCu_3Ti_4O_{12}$ sol-gel synthesized nanoparticle capacitors," *Journal of Advanced Dielectrics,* vol. 07, p. 1750017, 2017.

[7] R. Parra, R. Savu, L. A. Ramajo, M. A. Ponce, J. A. Varela, M. S. Castro, P. R. Bueno, and E. Joanni, "Sol–Gel synthesis of mesoporous $CaCu_3Ti_4O_{12}$ thin films and their gas sensing response," *Journal of Solid State Chemistry,* vol. 183, pp. 1209-1214, 2010.

[8] Y-S. Shen, C-C. Ho, and B-S. Chiou, "Impedance spectroscopy of $CaCu_3Ti_4O_{12}$ films showing resistive switching," *Journal of Electrochemical Society,* vol. 156, p. H466, 2009.

[9] L. C. Kretly, A. F. L. Almeida, P. B. A. Fechine, R. S. de Oliveira, and A. S. B. Sombra, "Dielectric permittivity and loss of $CaCu_3Ti_4O_{12}$ (CCTO) substrates for microwave devices and antennas," *Journal of Materials Science: Materials in Electronics,* vol. 15, pp. 657-663, 2004.

[10] H. S. Kushwaha, N. A. Madhar, B. Ilahi, P. Thomas, A. Halder, and R. Vaish, "Efficient solar energy conversion using $CaCu_3Ti_4O_{12}$ photoanode for photocatalysis and photoelectro-catalysis," *Scientific Report,* vol. 6, p. 18557, 2016.

[11] J-W. Lee, J-W. Lee, G-H. Lee, D-J. Shin, J. Kim, S-J. Jeong and J-H. Koh, "Ag-migration effects on the metastable phase in $CaCu_3Ti_4O_{12}$ capacitors," *Scientific Report,* vol. 8, p. 1392, 2018.

[12] J. A. Cortés, H. Moreno, S. Orrego, V. D. N. Bezzon, and M. A. Ramírez, "Dielectric and non-ohmic analysis of Sr^{2+} influences on $CaCu_3Ti_4O_{12}$-based ceramic composites," *Materials Research Bulletin,* vol. 134, p. 111071, 2021.

[13] A. A. Felix, V. D. N. Bezzon, M. O. Orlandi, D. Vengust, M. Spreitzer, E. Longo, D. Suvorov, and J. A. Varela, "Role of oxygen on the phase stability and microstructure evolution of $CaCu_3Ti_4O_{12}$ ceramics," *Journal of the European Ceramic Society,* vol. 37, pp. 129-136, 2017.

[14] P. Liu, P. Liu, Y. Lai, Y. Zeng, S. Wu and J. Han,"Influence of annealing conditions on microstructure and electrical properties of $CaCu_3Ti_4O_{12}$ (CCTO) ceramics," *Journal of Alloys and Compounds,* vol. 650, pp. 59-64, 2005.

[15] S. Rhouma, S. Rhouma, S. Saîd, C. Autret, S. De Almeida-Didry, M. El Amrani, and A. Megriche, "Comparative studies of pure, sr-doped, ni-doped and co-doped $CaCu_3Ti_4O_{12}$ Ceramics: Enhancement of dielectric properties," *Journal of Alloys and Compounds,* vol. 717, pp. 121-126, 2017.

[16] J. Jumpatam, B. Putasaeng, N. Chanlek, P. Kidkhunthod, P. Thongbai, S. Maensiri, and P. Chindaprasirt, "Improved giant dielectric properties of $CaCu_3Ti_4O_{12}$ via simultaneously tuning the electrical properties of grains and grain boundaries by F − Substitution," *RSC Advances,* vol. 7, pp. 4092-4101, 2017.

[17] K. Prompa, E. Swatsitang, and T. Putjuso, "Very low loss tangent and giant dielectric properties of $CaCu_3Ti_4O_{12}$ ceramics prepared by the sol–gel process," *Journal of Materials Scince: Materials in Electronics,* vol. 28, pp. 15033-15042, 2017.

[18] M. Chinnathambi, A. Sakthisabarimoorthi, M. Jose, and R. Robert, "Study of the electrical and dielectric behaviour of selenium doped CCTO ceramics prepared by a facile sol-gel route," *Materials Chemistry and Physics,* vol. 272, p. 124970, 2021.

[19] Y. Tian, X. Zhang, Y. Yang, Z. Liu, and X. Huang, "Sol-gel synthesis and sensing study of perovskite $CaCu_3Ti_4O_{12}$ nano-powders," *Integrated Ferroelectrics,* vol. 129, pp. 188-195, 2011.

[20] Sonia, M. Chandrasekhar, and P. Kumar, "Microwave assisted sol-gel synthesis of high dielectric constant CCTO and BFN ceramics for MLC applications," *Processing and Application of Ceramics,* vol. 11, pp. 154-159, 2017.

[21] J. Boonlakhorn, J. Prachamon, J. Manyam, P. Thongbai, and P. Srepusharawoot, "Origins of a liquid-phase annealing mechanism and giant dielectric properties of Ni+Ge Co-doped $CaCu_3Ti_4O_{12}$ ceramics," *Ceramics International,* vol. 47, pp. 13415-13422, 2021.

[22] O. Z. Yanchevskii, O. I. V'yunov, and T. O. Plutenko, "Carbonate precursor route for preparation of $CaCu_3Ti_4O_{12}$," *Ukrainian Chemistry Journal,* vol. 87, pp. 47-60, 2021.

[23] R. Kumar, M. Zulfequar and T. D. Senguttuvan, "Improved giant dielectric properties in microwave flash combustion derived and microwave annealed $CaCu_3Ti_4O_{12}$ ceramics," *Journal of Electroceramics,* vol. 42, pp. 41-46, 2019.

[24] H. Tang, H. Tang, Z. Zhou, C. C. Bowland and H. A. Sodano, "Synthesis of calcium copper titanate ($CaCu_3Ti_4O_{12}$) nanowires with insulating SiO_2 barrier for low loss high dielectric constant nanocomposites," *Nano Energy*, vol. 17, pp. 302-307, 2015.

[25] B. Samanta, P. Kumar, and C. Prakash, "Effect of annealing temperature and cu-rich secondary phase on dielectric properties of microwave processed $CaCu_3Ti_4O_{12}$ ceramics," *Ferroelectrics*, vol. 517, pp. 46–57, 2017.

[26] S. Pandey, V. Kumar, V. K. Sharma, and K. D. Mandal, "Effect of doping metal ions on microstructural evolution and dielectric behaviors of $CaCu_3Ti_4O_{12}$ Ceramics synthesized by semi-wet route," *Materials Chemistry and Physics,* vol. 253, p. 123384, 2020.

[27] L. Lin, Y. Liu, and M. Tian, "Enhancement of Breakdown electric field and dielectric properties of $CaCu_3Ti_4O_{12}$ ceramics

by Sr doping," *Materials Chemistry and Physics,* vol. 244, p. 122722, 2020.

[28] Y. Qu, Y. Wu, G. Fan, P. Xie, Y. Liu, Z. Zhang, J. Xin, Q. Jiang, and K. Sun, "Tunable radio-frequency negative permittivity of Carbon/$CaCu_3Ti_4O_{12}$ metacomposites," *Journal of Alloys and Compounds,* vol. 834, p. 155164, 2020.

[29] G. Wu, Z. Yu, K. Sun, R. Guo, X. Jiang, C. Wu, and Z. Lan, "Effect of $CaCu_3Ti_4O_{12}$ Dopant on the magnetic and dielectric properties of high-frequency MnZn power ferrites," *Journal of Magnetism and Magnetic Materials,* vol. 513, 167095, 2020.

[30] Z. Xu, D. Wang, and Z. Zhang, "Preparation and characterization of Mg^{2+}-doped $CaCu_3Ti_4O_{12}$ pigment with high NIR reflectance," *Ceramics International,* vol. 46, pp. 25306-25312, 2020.

[31] X. Yue, W. Long, J. Liu, S. Pandey, S. Zhong, L. Zhang, S. Du, and D. Xu, "Enhancement of dielectric and non-ohmic properties of graded co-doped $CaCu_3Ti_4O_{12}$ thin films," *Journal of Alloys and Compounds,* vol. 816, p. 152582, 2020.

[32] H. Lin, W. Xu, H. Zhang, C. Chen, Y. Zhou, and Z. Yi, "Origin of high dielectric performance in fine grain-sized $CaCu_3Ti_4O_{12}$ Materials," *Journal of European Ceramic Society,* vol. 40, pp. 1957-1966, 2020.

[33] S. Pongpaiboonkul, T. M. Daniels, and S. K. Hodak, "Preferentially oriented fe-doped $CaCu_3Ti_4O_{12}$ films with high dielectric constant and low dielectric loss deposited on $LaAlO_3$ and $NdGaO_3$ substrates," *Applied Surface Science,,* vol. 540, p. 148373, 2021.

[34] S. Li, J. Zhang, S. Jamil, Q. Cai, and S. Zang, "Conversion of eggshells into calcium titanate cuboid and its adsorption properties," *Research on Chemical Intermediates*, vol. 44, pp. 3933-3946, 2018.

[35] A. Maddu, N. F. Wahyuni, and Irmansyah, "The Effect of annealing temperature on structure and electrical properties of $CaTiO_3$ synthesized from Hen's Eggshell via hydrothermal process," *International Journal of Nanoelectronics and Materials,* vol. 12, no. 3, pp. 257-264, 2019.

[36] K. Maitreekeaw, and T. Chanadee, "Calcium Titanate ceramics obtained by combustion synthesis and two-step annealing," *Science of Annealing,* vol. 52, pp. 491-502, 2020.

[37] K. W. Goh, D-J. Lin, H-L. Lin, S-M. Haung, S-M. Liu, and W-C. Chen, " Effect of PH on the properties of eggshell-derived hydroxyapatite bioceramic synthesized by wet chemical method assisted by microwave irradiation," *Ceramics International,* vol. 47, pp. 8879-8887, 2021.

[38] A. Ashokan, A. Ashokan, V. Rajendran, T. S. S. Kumar, and G. Jayaraman, "Eggshell derived hydroxyapatite microspheres for chromatographic applications by a novel dissolution - precipitation method," *Ceramics International,* vol. 47, pp. 18575-18583, 2021.

[39] D. Muthu, G. S. Kumar, V. S. Kattimani, V. Viswabaskaran, and E. K. Girija, "Optimization of a lab scale and pilot scale conversion of eggshell biowaste into hydroxyapatite using microwave reactor," *Ceramics Interntional,* vol. 46, pp. 25024-25034, 2020.

[40] S. Cherdchom, T. Rattanaphan, and T. Chanadee, "Calcium titanate from food waste: combustion synthesis, annealing, characterization, and properties," *Advances in Materials Science and Engineering,* vol. 2019.

[41] D. P. Samarakoon, and R. N. Singh, "Thickness dependent dielectric properties of calcium copper titanate ceramics measured in a controlled atmosphere," *Ceramics International,* vol. 45, pp. 16554-16563, 2019.

[42] Y. Li, W. Li, G. Du, and N. Chen, "Low Temperature preparation of $CaCu_3Ti_4O_{12}$ ceramics with high permittivity and low dielectric loss," *Ceramics International,* vol. 43, pp. 9178-9183, 2017.

[43] D. S. Tsai, D. S. Tsai, T. S. Chin, S. E. Hsu, and M. P. Hung, "A simple method for the determination of lattice parameters from powder x-ray diffraction data," *Materials Transactions, JIM,* vol. 30, no. 7, pp. 474-479, 1989.

[44] S. Jesurani, S. Kanagesan, and T. Kalaivani, "Phase formation and high dielectric constant of calcium copper titanate using sol-gel route," *Journal of Materials Science: Materials in Electronics,* vol. 23, pp. 668-674, 2021.

[45] S. F. Shao, J. L. Zhang, P. Zheng, W. L. Zhong, and C. L. Wang, "Microstructure and electrical properties of $CaCu_3Ti_4O_{12}$ ceramics," *Journal of Applied Physisics,* vol. 99, p. 084106, 2006.

[46] J. Mohammed, T. T. C. Trudel, H. Y. Hafeez, B. I. Adamu, Y. S. Wudil, Z. I. Takai, S. K. Godara, and A. K. Srivastavaa, "Tuning the dielectric and optical properties of Pr Co–substituted calcium copper titanate for electronics applications," *Journal of Physics and Chemistry of Solids,* vol. 126, pp. 85-92, 2019.

[47] X. Li, J. Wang, H. Chen, C. Xiong, Z. Shi, and Q. Yang, "Flexible dielectric nanocomposite films based on Chitin/ Boron Nitride/Copper calcium titanate with high energy density," *Composites Part A, Applied Science and Manufacturing,* vol. 149, p. 106554, 2021.

[48] B. S. Prakash, and K. B. R. Varma, "Influence of annealing conditions and doping on the dielectric relaxation originating from the surface layer effects in $CaCu_3Ti_4O_{12}$ ceramics," *Journal of Physics and Chemistry of Solids,* vol. 68, pp. 490-502, 2007.

[49] P. Thongbai, Y. Teerapon, M. Santi, A. Vittaya, C. Prinya, and D. Damjanovic, "Improved dielectric and nonlinear electrical properties of fine-grained $CaCu_3Ti_4O_{12}$ ceramics prepared by a glycine-nitrate process," J*ournal of the American Ceramics Society*, vol. 97, no. 6, pp. 1785-1790, 2014.